Materials and Methods

Plasmids

The TPR domain of KLC2 ($KLC2^{TPR}$, amino acids V218 to K480) was amplified from a mouse template and subcloned into the NdeI/XhoI sites of the pET28a vector (Novagen) to enable its expression with a thrombin-cleavable N-terminal hexa-histidine tag. To generate the chimeric protein used for crystallization the first W-acidic motif of SKIP ($SKIP^{WD}$) was fused to the N-terminus of $KLC2^{TPR}$ via a $(TGS)_4$ linker. The oligonucleotides, SKIPKBSFOR–
TATGaccaacctggagtgggatgacagtgcgattACGGGGAGTACGGGGAGTACGGGGAGT
ACGGGGAGTCA and SKIPKBSREV–
TATGACTCCCCGTACTCCCCGTACTCCCCGTACTCCCCGTaatcgcactgtcatcccac
tccaggttggtCA, were annealed together and the double-stranded DNA inserted into the NdeI site of the pET28a-KLC2TPR plasmid. CB6-GFP-SKIP(1-310) and CB6 HA-KLC2 were described previously (*7*). CB6-GFP-CSTN (879-971) was amplified by PCR from IMAGECLONE 100003893 (Source Biocience, Nottingham) and cloned into CB6-GFP.

Mutation of the WD and WE doublets in the first and second W-acidic SKIP motifs to AA in CB6-GFP-SKIP and binding site mutations into KLC2 were made using the Quickchange system (Stratagene). Wild-type and mutant KLC2 sequences were subcloned into CB6-GFP as required. The fidelity of all constructs was verified by sequencing.

Protein expression and purification

Proteins were expressed in *E.coli* BL21(DE3) cells. Briefly, single colonies were picked and grown at 37 °C overnight. Small-scale overnight bacterial cultures was used to inoculate 4x1L cultures that were incubated at 37 °C until they reached an OD600 of 0.5. The temperature was then lowered to 16 °C and protein synthesis was induced by the addition of 300 μM IPTG for 16 hours. Cells were harvested by centrifugation at 5000 g for 15 minutes at 4 °C and resuspended in 25mM HEPES pH 7.5, 500mM NaCl, 20mM imidazole, 5mM β-mercaptoethanol supplemented with protease inhibitor cocktail (Roche). Cell lysis was accomplished by sonication. Insoluble material was sedimented by centrifugation at 16500 g for 1 hour at 4 °C and the supernatant filtered using 0.22 μm prior to loading on a His-trap HP column (GE Healthcare) pre-equilibrated with lysis buffer. The $SKIP^{WD}$- $KLC2^{TPR}$ chimera was eluted with an imidazole gradient and fractions containing the target protein collected and dialysed overnight against imidazole-free lysis buffer. The sample was further purified by size-exclusion chromatography (SEC) on a 16⁄60 HiLoad Superdex 75 column (GE Healthcare). $KLC2^{TPR}$ lacking the $SKIP^{WD}$ fusion used for biophysical measurements was prepared in a similar manner.

Crystallization and structure determination

The $SKIP^{WD}$- $KLC2^{TPR}$ chimera was concentrated to 4.8 mg⁄ml in storage buffer (25mM HEPES pH 7.5, 500mM NaCl, 5mM β-mercaptoethanol). Crystallization was achieved by the vapour diffusion set-up at 18 °C in 400 nl sitting drops dispensed with the aid of Mosquito crystallization robot (TTP LabTech). Reproducible crystal hits were obtained employing the tagged version of the chimera in the poly-γ-glutamic acid (PGA) screen (*22*) (Molecular Dimensions) and also in ammonium sulphate based conditions of the ProComplex screen (Qiagen). Removal of the tag by proteolytic cleavage had a negative impact on crystallization. Optimised crystals were

obtained using 0.10 M Mes pH 6.5, 0.2 L-proline, 7% PGA. For data collection crystals were dehydrated/cryoprotected by soaking them in 3.6 M ammonium sulphate, 0.10 M MES pH 6.5 for 90 minutes. A complete dataset was collected at 2.9 Å resolution at the I24 beamline of Diamond Light Source (Didcot, Oxford, UK). Data were processed with *xia2* (*23*) using XDS (*24*) and SCALA (*25*) packages. Crystals belong to space group $P2_12_12$ with cell dimensions a = 87.81 Å, b = 90.86 Å, c = 94.04 Å. The structure was determined using the molecular replacement technique using the program MOLREP (*26*) and employing the structure of apo $KLC2^{TPR}$ (PDB code 3CEQ) as search model. An initial search allowed the positioning of the expected two $KLC2^{TPR}$ molecules. However, clashes and poor density for the N-terminal region of the molecule suggested this region to be different from the search model. We then repeated the rotational/translational search using a model encompassing TPR4-6 only. This produced a clear solution characterized by high contrast. Electron density maps calculated following cycles of rigid-body and NCS-restrained atomic refinement using TLS modelling with REFMAC5 (*27, 28*) and BUSTER (*29*) allowed to model the TPR2-3 region in the $SKIP^{WD}$-$KLC2^{TPR}$ in chimera as well as the bound $SKIP^{WD}$ cargo peptide. Model building was performed using COOT (*30*). Simulated-annealing omit maps were calculated with CNS (*31*) The quality of the final models was assessed with the program MOLPROBITY (*32*). A summary of data collection and refinement statistics are shown in Table S1. Structural images were prepared with PyMol (DeLano Scientific, LLC).

Fluorescence polarization

N-terminal carboxytetramethylrhodamine (TAMRA) conjugated peptides used for fluorescence polarization measurements $SKIP^{WDWE}$: TAMRA-STNLEWDDSAIAPSSEDYDFGDVFPAVPSVPSTDWEDGDL, $SKIP^{WD}$: TAMRA-STNLEWDDSAI, $SKIP^{WE}$: TAMRA-VPSTDWEDGDL, $CSTN^{WD1}$: TAMRA-ENEMDWDDSAL, $CSTN^{WD2}$: TAMRA-QQQLEWDDSTL were supplied by BioSynthesis (Lewisville, TX, USA). Measurements were performed on a Horiba Fluoromax-4 spectrofluorometer at 20 °C by incubating 100 nM TAMRA-labeled peptides with $KLC2^{TPR}$ at increasing concentrations in 25 mM Hepes pH 7.5, 5 mM β-mercaptoethanol and NaCl ranging from 75 mM to 500 mM. Data analysis was performed using the Prism (GraphPad Software Inc., San Diego CA, USA) package.

Cell Culture, transfection and immunoprecipitation

Cell culture was carried out as described previously(*33*). To analyse the interaction between SKIP KLC-binding proteins and KLC, a 10-cm dish of HeLa cells at 70% confluency was co-transfected with CB6 expression vectors encoding GFP-SKIP 1-310 and HA-tagged mouse KLC2. After 16 h, transfected cells were lysed in 1ml of 25 mM HEPES pH 7.5, 150 mM NaCl, 0.5% NP-40, 0.5X Triton-X 100 containing a protease inhibitor cocktail (Roche) for 10 mins prior to centrifugation at 13 000 g for 10 min at 4C. The resulting supernatant was incubated with 15µl of prewashed GFP-Trap beads for 90 minutes. 50µl of supernatant was retained for analysis of input HA-KLC2 levels (20µl loaded). Beads were washed 4x and boiled in 60ul SDS- loading buffer (30µl loaded). Samples were subjected to SDS–PAGE and analyzed by western blot using antibodies against GFP and HA.

Immunofluoresence

HeLa cells on fibronectin-coated coverslips were co-transfected with plasmids encoding Arl8b-HA, myc-SKIP and GFP-KLC2 (wild-type or mutants). After 16

hours, cells were fixed and stained with the indicated combinations of a polyclonal anti-HA antibody (Sigma), anti-Myc (9E10) and LAMP-1 (H4A3, Developmental Studies Hybridoma bank). Immunofluorescence images were collected using a Zeiss Olympus IX-81 microscope (Metamorph, Sutter filter wheels, ASI X-Y stage, Photometrics CascadeII 512B camera with a 100x UPlanApoS NA1.4 objective). Figures were assembled using the Adobe Photoshop and Illustrator packages (Adobe, CA, USA).

Supplementary text

Structure of SKIP^{WD}-KLC2^{TPR}

The deposited SKIP^{WD}-KLC2^{TPR} model comprises two SKIP^{WD} chains (X and Y) and two KLC2^{TPR} chains (A and B) arranged in two complexes (X:A and Y:B) related by a two-fold NCS (Fig S2). The $(TGS)_4$ linker used to fuse the SKIP^{WD} peptide to the KLC2^{TPR} domain is not visible in electron density maps. Thus, we cannot establish whether the crystallographic complexes result from an intermolecular or intramolecular binding event. In addition to the $(TGS)_4$ linker, other regions exhibit limited or no electron density. These include the N-terminal hexahistidine tag and its downstream thrombin cleavage site, the external TPR1 helix of and part of the long connector linking TPR5 to TPR6.

Secondary structure matching between apo and cargo-loaded KLC2^{TPR} gives a rmsd of 2.0 Å for 226 residues aligned. This value decreases to 0.64 Å when only the TPR4-TPR6 segment (residues 317-479) is used in the structural alignment. With respect to this invariant reference frame the movement of TPR2-3 is that of a rigid jaw which closes upon cargo recognition engendering the binding surface and pockets for the SKIP^{WD} peptide. A similar comparison between apo KLC1^{TPR} (3NF1) and cargo-loaded KLC2^{TPR} reveals less deviant overall conformations (rmsd of 1.56 Å for 212 aligned residues). Interestingly, the His-tag of KLC1^{TPR} fortuitously occupies part of the W-acidic binding groove in that structure (Fig. S3). Overall, it appears that binding in this region of the TPR domain favours a closure of the TPR2-3 region relative to the rest of the molecule.

The most important features of the SKIP^{WD}:KLC2^{TPR} interface are given in the main text. Here we describe additional aspects. Structurally, a leucine residue at *p*-2 appears an important contributor to the stability of the complex. Consistent with this, mutational alanine scanning using the second W-acidic motif of calsyntenin showed *p*-2 leucine to be the only residue essential for recognition by KLC1 in addition to W(*p*0)D(*p*+1) (*12*) . The low affinity SKIP^{WE} motif displays a threonine residue at *p*-2. Residues at positions p-(3,4) are less important for complex stability although they likely play a modulatory role. An H-bond is present between the main chain carbonyl oxygen of SKIP^{T203} and the amide side-chain of N336 suggesting that these positions can accommodate alternative side chains. This is consistent with their general lack of sequence conservation amongst W-acidic motif cargo (*7*). The C- terminal stretch of SKIP^{WD} encompassing *p*+(2,3,4,5) is observed in a more compact, turn-like conformation with SKIP^{D209,S210} at p+(2,3) making very minor contacts with the groove. As an acidic residue at *p*+2 is a common feature of the W-acidic motif we wondered whether its stabilization could be provided by TPR1 in a complete KLC^{TPR}. Indeed, the super-helical geometry of TPR domains suggests the latter could have a role in stabilizing this region of the motif (Fig. S3). However, TPR1 has been found to be dispensable for Calsyntenin "WD" motif-dependent initiation of kinesin-1 activation in vivo (*12*) suggesting an ancillary role for this repeat. Consistent with our structural results the same study also found TPR6 unnecessary. Finally, SKIP^{A211,I212} at p+(4,5) interact with N244, I245, L248 and R270 of TPR2 and A283 of TPR3 with good shape complementarity. An H-bond between the carbonyl oxygen of SKIP^{A211} and R251 stabilizes the turn. As for the N-terminal peripheral region of SKIP^{WD} the exact nature of the amino acids at *p*+(4,5) does not seem critical for complex stability. Alternative side-chains can be positioned at this topological position possibly

involving a rearrangement of the main-chain. This is in line with the high sequence variability within W-acidic motifs at sites away from the *p*-2:p+2 core.

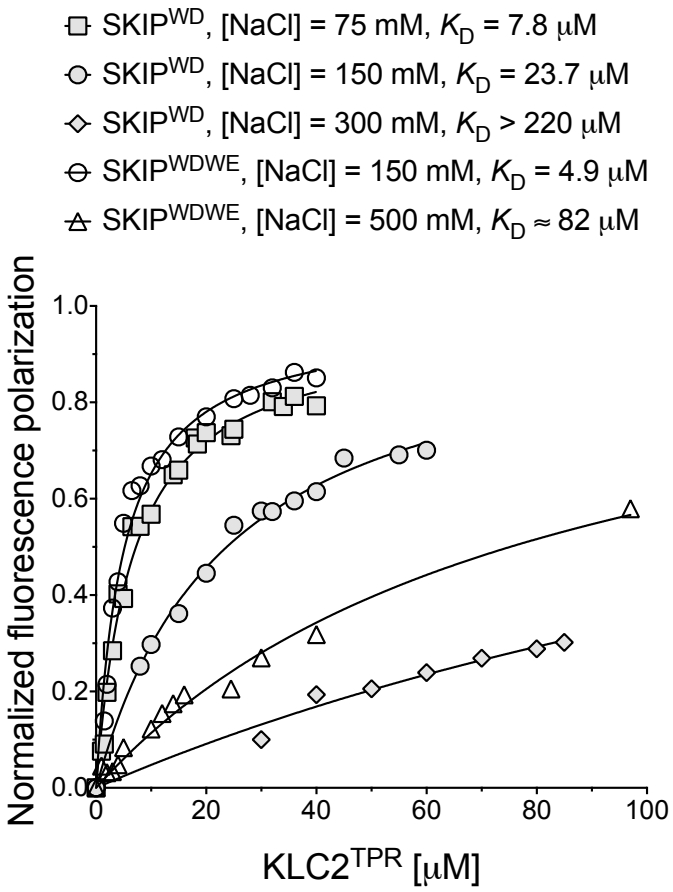

Figure S1.

Fluorescence polarization measurements at variable ionic strength. Polarization measurements were carried out using a fluorescent version of the $SKIP^{WDWE}$ and $SKIP^{WD}$ peptides at the stated NaCl concentrations as described in Materials and Methods. The strong dependence of the binding affinity on the salt concentration indicates that electrostatics plays a critical role in the kinesin-cargo interaction.

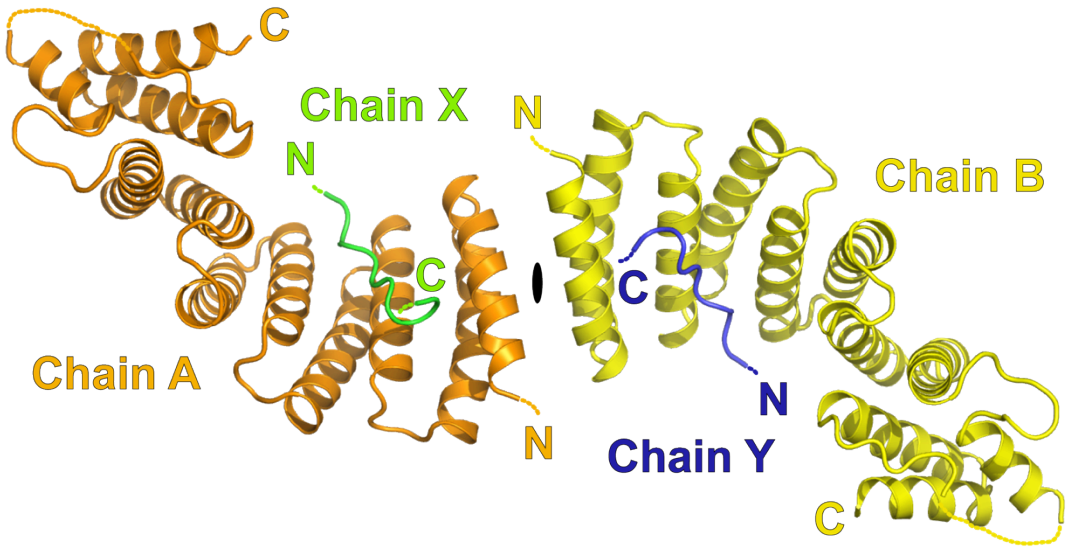

Figure S2

Organization of the SKIP^{WD}-KLC2^{TPR} dimer. Chains X and Y for the SKIP^{WD} peptides are shown in green and blue, respectively. Chains A and B for the KLC2^{TPR} domains are shown in orange and yellow, respectively. A two-fold NCS indicated by the black oval relates X:A and Y:B complexes.

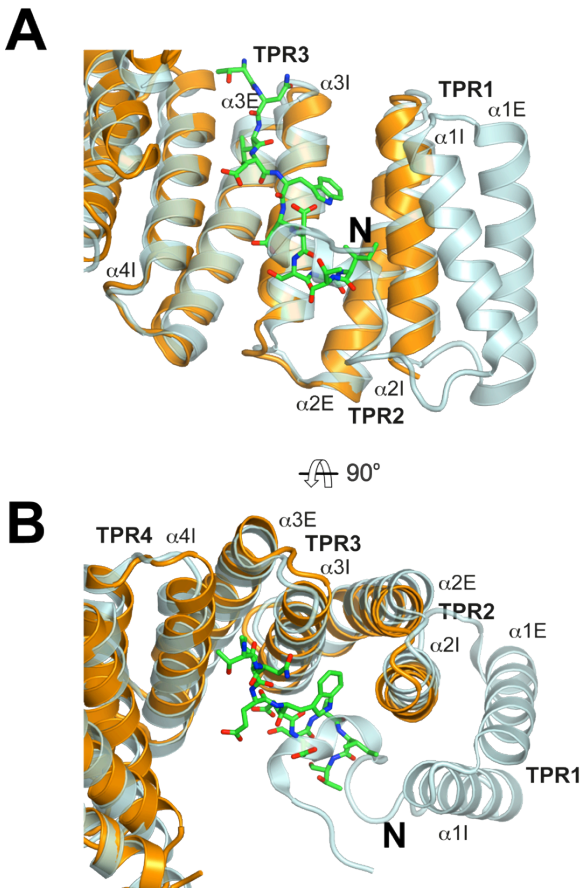

Figure S3

(A, B) Orthogonal views of KLC1^{TPR} (PDB code 3NF1) superposed to the SKIP^{WD}-KLC2^{TPR} complex. KLC2^{TPR} and KLC1^{TPR} are shown as orange and light blue cartoons, respectively, with TPR1-4 and their constituting helices labelled. The model for the SKIP^{WD}-KLC2^{TPR} cargo complex does not include TPR1. The SKIP^{WD} cargo peptide is shown as stick representation in green. The N-terminal purification tag of KLC1^{TPR} partly overlaps with the cargo binding site and suggests that perhaps that binding in this region of the TPR domain favors a closure of the TPR2-3 region relative to the rest of the molecule. The superposition also suggests that although not essential, the internal TPR1 helix (α1I) might contribute to the stabilization of W-acidic motifs.

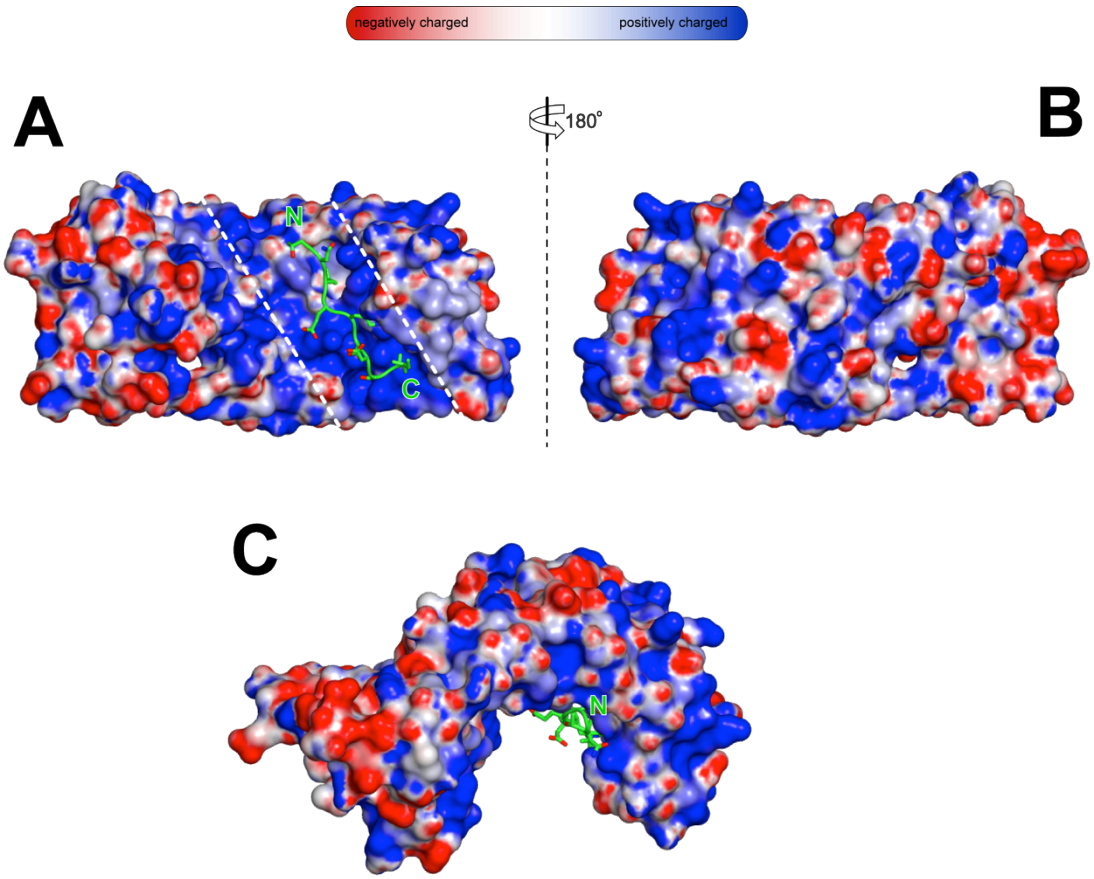

Figure S4

The W-acidic cargo motif binds in the positively charged groove of the TPR domain. Front **(A)**, back **(B)** and top **(C)** views of the SKIP^{WD}-KLC2^{TPR} complex. KLC2^{TPR} is shown as surface representation colored by its electrostatic potential. The SKIP^{WD} peptide is shown as a green tube with stick side chains. Top view in (C) is approximately along the axis of the SKIP^{WD}. The cargo peptide binds mostly in an extended conformation in the positively charged inner concave surface of the TPR domain. In (A) the binding grove is highlighted by two white dashed lines.

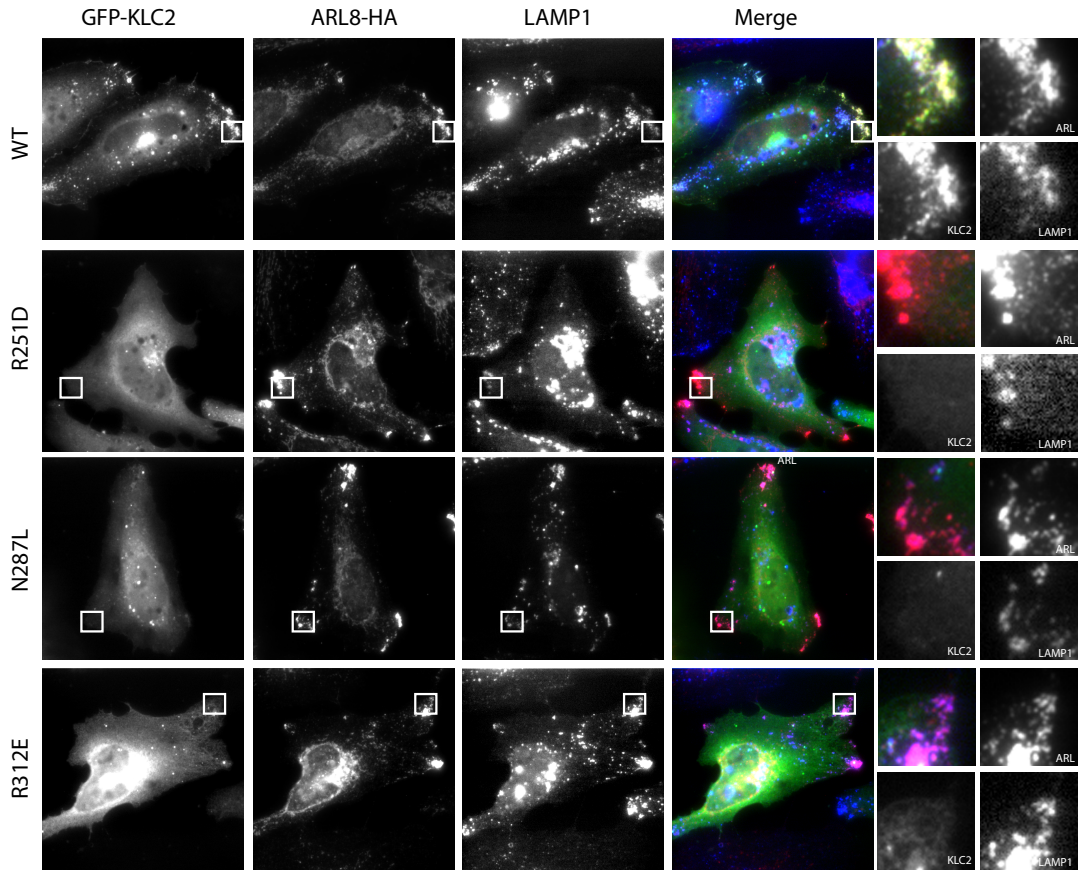

Figure S5

Replacement of key KLC2^{TPR} residues results in loss of GFP-KLC2 association with Arl8/LAMP-1 positive lysosomal membranes. In merge panels, GFP-KLC2, Arl8 and LAMP-1 are shown in green, red and blue respectively.

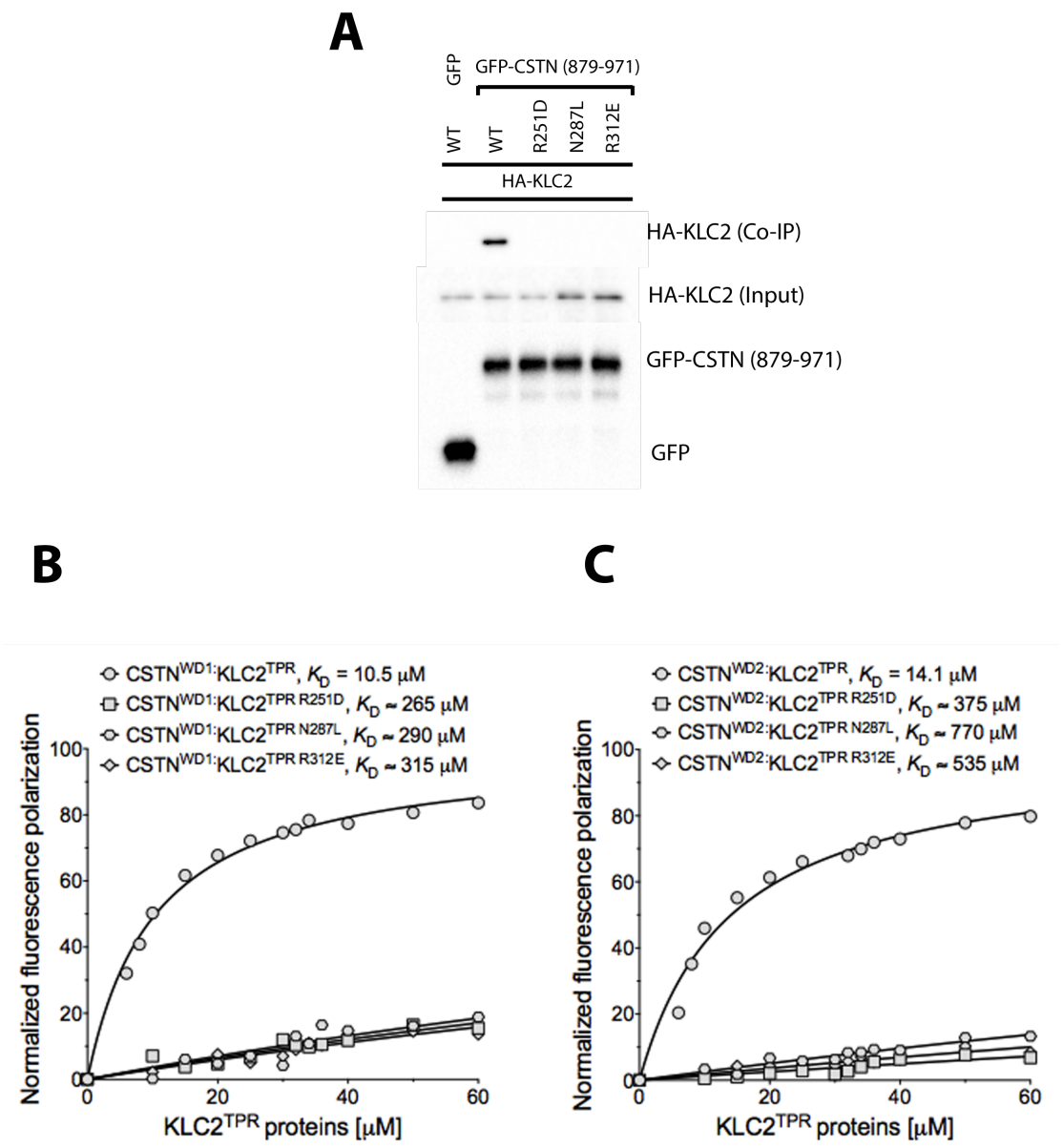

Figure S6

KLC2^{TPR} mutations affecting SKIP binding also affect binding to Calsyntenin. (**A**) Co-immunprecipation assay showing the effect of KLC2^{TPR} mutations on the interaction with the cytoplasmic domain of Calsyntenin (CSTN, residues 879-971). Binding is abrogated by all of the mutations shown. (**B, C**) Fluorescence polarization measurements showing binding affinity of CSTN^{WD1} (**B**) and CSTN^{WD2} (**C**) with KLC2^{TPR} and the indicated mutated forms. Both peptides interact with KLC2^{TPR} with similar affinity comparable to SKIP^{WD} (Figure 3B). Mutations in the interface that we have defined as for SKIP^{WD} essentially abrogate binding.

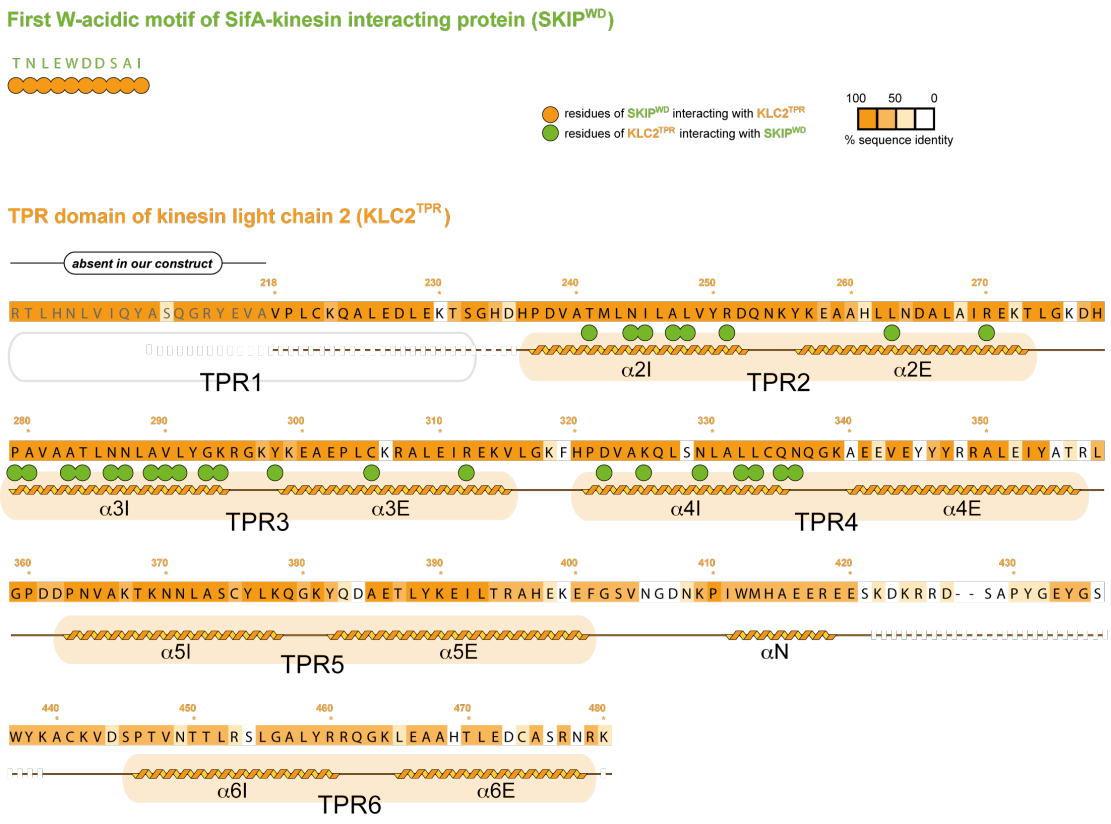

Figure S7

Sequence and secondary structure of the SKIP^{WD} and KLC2^{TPR} domains. Colored circles show residues of one domain contacting the other (*19*) as indicated in the inset. Amino acids of the KLC2^{TPR} domain are color-coded according to sequence conservation within the KLC(1-4) family as highlighted by the conservation bar. All KLC2^{TPR} residues involved in binding the W-acidic motif are totally conserved.

Table S1.

Data collection and refinement statistics.

Data set	$SKIP^{WD}$-$KLC2^{TPR}$
Data collection	
Beamline	I24 (DLS)
Wavelength (Å)	0.9686
Resolution range (Å)/Highest res. bin (Å)	52.42-2.90/(2.98-2.90)
Space group	$P2_12_12$
Cell dimensions (Å)	87.81, 90.86, 94.04
Unique reflections	17034
Overall redundancy	5.60/(5.04)
Completeness, (%)	99.0/(98.2)
Wilson B ($Å^2$)	95.4
R_{symm} (%)	7.1/(70.0)
$\langle I/\sigma(I) \rangle$	10.5/(2.4)
Refinement	
PDB code	3ZFW
R_{factor} (%)/R_{free}(%)	20.27/24.48
# non-H atoms	3751
Mean B value ($Å^2$)	108.7
rmsd bond lengths (Å)	0.009
rmsd bond angles (°)	1.03
Molprobity score	1.89 (99% percentile)